



# Imaging fields around growing crystals

A.G. Notcovich, I. Braslavsky, S.G. Lipson\*

*Physics Department, Technion – Israel Institute of Technology, Haifa 32000, Israel*

---

## Abstract

Crystal growth morphologies arise from the interplay between interface mechanisms and temperature or concentration fields around the growing crystal. We shall describe experimental methods which we have developed in order to measure these fields in both two- and three- dimensional environments. We compare the observations with current growth theories for examples of two distinctly different types of crystal. The first example is  $\text{NH}_4\text{Cl}$ , a cubic crystal which grows dendritically from supersaturated aqueous solution, in which we have measured the two-dimensional concentration field by interference microscopy. The experiments allow determination of the anisotropies of both the surface tension and the kinetic growth admittance. As a result we have been able to explain the morphological transition observed in this crystal at high growth velocities. The second example is heavy ice ( $\text{D}_2\text{O}$ ) growing from supercooled heavy water, in which we have investigated the three-dimensional temperature field by interference tomography. Ice crystals are very anisotropic and show peculiar growth modes. We illustrate the use of the temperature map in understanding the stability of asymmetrical morphologies which have been observed in ice and other crystals. © 1999 Elsevier Science B.V. All rights reserved.

*Keywords:* Imaging fields; Interference microscopy; Morphology; Tomography

---

## 1. Introduction

The shapes and symmetries of crystals have always delighted and intrigued mankind. There are basically two families of crystal shapes: equilibrium shapes and growth shapes. Although both result from the same underlying crystal structure and

symmetry, they have different origins. The equilibrium shape is determined by minimizing the total surface energy of the crystal, and can be described completely in terms of the surface free energy  $\gamma(\theta, \phi)$ . The mathematical problem relating the shape and  $\gamma$  was solved by Wulff [1,18]; it is usually described by a mathematical construction (the Wulff construction) which has many curious and intriguing properties and has been analyzed in detail by Herring [2]. The construction leads to a one-to-one correspondence between crystal properties and shape. However, true equilibrium shapes

---

\* Corresponding author. Fax: +972 4 822 1514; e-mail: [sglipson@physics.technion.ac.il](mailto:sglipson@physics.technion.ac.il).

are rarely observed in reality, and although this problem has in the past led to some exciting physics it is today of limited interest. The growth shapes of crystals show a different picture. A given crystal can have different morphologies depending on its rate of growth and its history, and other parameters, not just  $\gamma$ , are involved. These shapes are generally the ones which are observed (even in geology, where one might think that enough time has elapsed for equilibrium to be obtained!), but their explanation in terms of basic physics has been elusive.

There are several different processes which are relevant to the growing crystal, and the complication of the problem essentially arises because these processes can be mixed in different proportions. In the case of a crystal growing from a supercooled melt, we can list the following: diffusion of latent heat away from the growing crystal–melt interface, atomic or molecular attachment kinetics at the interface, local deviation from equilibrium at the interface resulting from curvature (Gibbs–Thomson effect). It is possible to write down equations representing each of these processes in a more or less realistic manner, and to try to solve them together to find the interface position as a function of time. Even if each of the processes itself is represented by a linear approximation, the resulting problem is highly non-linear, because of the moving interface. As a result, there are often situations in which small fluctuations grow exponentially and become dominant in the long run.

Much effort has been put into the search for stationary solutions to the problem, in which a given interface shape translates linearly with time, since such solutions are usually selected by experimental systems. It has been found in general that stationary solutions can be classified into groups which appear morphologically different from one another. Examples are crystalline dendrites (branching crystals which show strongly directional properties), symmetry-broken dendrites (which grow isotropically in pairs, called “doublons” in two dimensions and triads “triplons” in three dimensions, in which each element provides a stable environment for the others), faceted crystals and others. In each case theoretical frameworks have been constructed, either analytically [3,4] or numerically [5,6]. It has recently appeared from the-

oretical work that the different growth modes appear in fairly well-defined regions of a phase diagram whose parameters are normalized supercooling ( $\Delta$ ) and anisotropy of surface tension ( $\gamma(\theta)$ ) and of kinetic growth admittance ( $\beta(\theta)$ ) [7].

The work described in this paper is an attempt to connect these theoretical ideas with real life. Clearly, the shape (morphology) of a crystal, growing in a medium whose global supercooling alone is known, does not tell the complete story. We should like to determine its interface parameters and to relate these to the growth modes observed. In addition, we should like to compare the driving fields calculated in theoretical models with those obtained in the experiment. To do this, we have developed optical techniques to image the concentration and temperature fields in two and three dimensions, and from their behavior at the interface to learn as much as possible about the parameters relevant to the models.

## 2. Interference microscopy and tomography

The techniques which we have developed are based on the temperature and concentration dependence of refractive index of a transparent fluid. The refractive index field  $n(x, y, z)$  is measured by interference techniques [8,9]. The experiments use different types of interferometer for this purpose. In one variation [10], a quasi two-dimensional optical cell of thickness  $Z$  is situated in a Linnik interference microscope (variant of the Michelson interferometer) and the optical thickness of the cell is measured as a function of the position in the image (see Fig. 1). The optical thickness for a double pass through the object can be represented as a phase difference  $\phi(x, y)$  with respect to the value  $\phi_0(x, y)$  at the same point in an empty cell

$$\phi(x, y) - \phi_0(x, y) = \frac{4\pi}{\lambda} \int_0^Z n(x, y) - n_0(x, y) dz. \quad (1)$$

Using computer-based image processing [10] it is possible to determine the phase at each pixel to an accuracy of about 0.03. In order to get good imaging, the thickness  $Z$  cannot be much larger than the

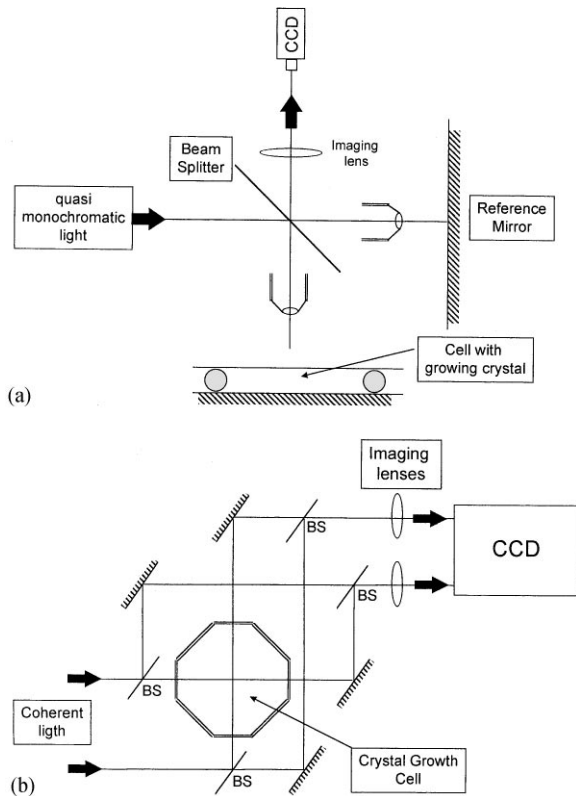


Fig. 1. Schematic diagrams showing the optics used in the experiments: (a) Linnik interference microscope, (b) Optical tomography using Mach-Zehnder interferometers (only two interferometers are shown).

depth of focus of the microscope, so that this method is limited to rather thin cells; the examples shown in this article refer to a cell 11  $\mu\text{m}$  thick. Because the cell walls are approximate isotherms, this two-dimensional method is mainly applicable to growth from solution, where the concentration field is measured under isothermal conditions. A concentration resolution of about 0.01% with a spatial resolution of 1  $\mu\text{m}$  has been achieved.

The second technique which we have used is interferometric tomography [11]. This is an extension of the above idea to three-dimensional fields. The object is situated in the line of sight of four interferometers, each with its axis in a different spatial direction, which carry out integrals of the form of Eq. (1) along their axes. The output is a set of projections of  $n(x, y, z)$ . Using tomographic tech-

niques developed specially for a limited set of projections [12], we derive the full three-dimensional function  $n(x, y, z)$ . We have used this method to investigate the temperature fields around crystals growing from the melt; such experiments cannot be done in the thin two-dimensional cells because the walls disturb the temperature field. These experiments are macroscopic in scale; a temperature resolution of about 0.05°C has been achieved with a spatial resolution of about 0.5 mm.

### 3. Growth in two dimensions: ammonium chloride growing from supersaturated solution

We have used ammonium chloride as an example for solution growth because the crystals are quite anisotropic in their growth and because morphological transitions between growth along  $\langle 100 \rangle$ ,  $\langle 110 \rangle$  and  $\langle 111 \rangle$  with increasing  $\Delta$  have been observed [13]. Models for transitions between growth morphologies have been described by Ben-Jacob et al. [14] and Brener [15] and are based on competition between differing anisotropies of  $\gamma$  and  $\beta$ . For reasons of conservation of matter, growth occurs fastest where the normal concentration gradient at the interface is greatest, from which it follows that the anisotropy of  $\gamma$  dominates at low growth velocities and that of  $\beta$  at high velocities. We report here a series of experiments at various growth velocities (controlled by  $\delta$ ) which are illustrated in Fig. 2. Under conditions where the growth is in  $\langle 100 \rangle$  the interface can clearly be determined and the concentration (and hence local supercooling  $\Delta_i$ ) determined at each point on it. Now the local supercooling is made up of two contributions. The first is the Gibbs–Thomson curvature effect

$$\Delta_G = \kappa(\gamma + \gamma''), \quad (2)$$

where  $\kappa$  is the local curvature of the interface and  $\gamma'' \equiv d^2\gamma/d\theta^2$  in two dimensions. The second is the kinetic growth resistance

$$\Delta_K = \beta(\theta)v_{\perp} \quad (3)$$

in which  $v_{\perp}$  is the growth velocity component normal to the interface. The normal concentration gradient is generally largest at points where the

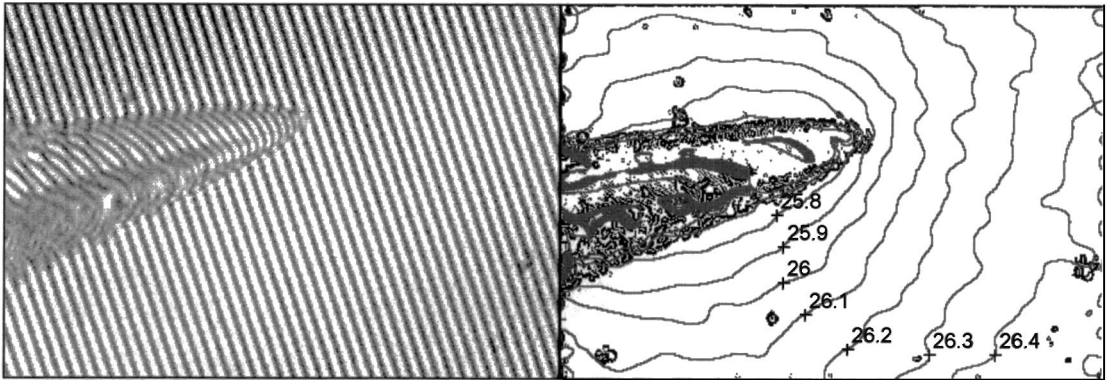


Fig. 2.  $\text{NH}_4\text{Cl}$  growing in the  $\langle 100 \rangle$  direction. (a) typical interferogram, (b) concentration map.

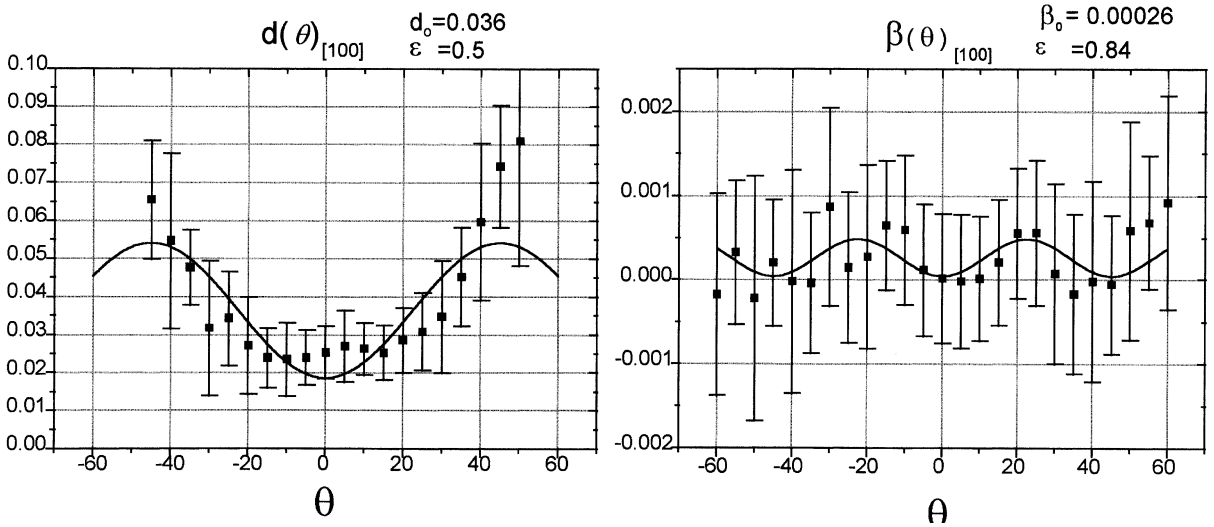


Fig. 3. The capillary length  $d_0$  and the growth admittance  $\beta$  measured as a function of angle  $\theta$  from the  $\langle 100 \rangle$  axis. The data has been fitted to sinusoidal functions of the angle to emphasize the periodicity.

sum of Eqs. (2) and (3), the total supercooling of the fluid at the interface, is smallest. Such points would be expected to grow fastest and their orientations to be selected, but a complete solution of the field equations for the whole system is necessary to justify this statement exactly.

From the determination of the crystal interface profile (which, incidentally, is well represented by a parabola near to the growth tip) and the concentration field measurements as a function of growth velocity it is straightforward to determine  $\beta(\theta)$  and

$(\gamma + \gamma'')(\theta)$ . A preliminary analysis of the results is shown in Fig. 3. One should note that the error-bars of  $\beta(\theta)$  are very large. When the two contributions  $\Delta_G$  and  $\Delta_K$  (Eqs. (2) and (3)) are added together, the minimum of the combined function is at angle  $\theta = 0$  for small growth velocities, but at larger velocities the second minimum at  $\theta = 50^\circ$  becomes dominant, and this explains rather nicely the observed change in growth axis to  $\langle 111 \rangle$ .

Continuation of these experiments to crystals growing in the  $\langle 111 \rangle$  direction is not possible,

because the assumption of a continuous interface profile, on which definition of  $\kappa$  is based, breaks down. Careful microscopic examination of the tip reveals that it comes to a tip which is apparently discontinuous (sharp) on the scale of the resolution of the microscope [16]. In this case, many possible orientations  $\theta$  are not represented.

In general, when the growth velocity is high, we can neglect the capillary correction (2) and represent  $\Delta_i$  by  $\Delta_\kappa$  alone (3). Now when the crystal grows, its steady-state shape can be represented by a Wulff construction on the  $v(\theta)$  polar diagram [17,19]. This result follows if we consider each point on the interface as the crystal grows for a time  $\delta t$ . Its new position will be given by moving the

interface to a point on a plane parallel to the interface a distance  $v(\theta)\delta t$  from it in the direction of growth. This was shown by Frank (see Refs. [17,19]) to give a Wulff construction in which the generating function is a polar plot of  $v(\theta)$ . It is well known in the study of equilibrium crystal shapes [2] that if the generating function is sufficiently anisotropic, some surface orientations will be missing. Likewise, if  $v(\theta)$  is sufficiently anisotropic, the fastest-growing orientations “grow out” of the crystal, whose shape becomes dominated by the slowest-growing orientations (often, but not always, facets). A simple geometrical interpretation which allows us to see when this happens is shown in Fig. 4; as far as we know, this is the first

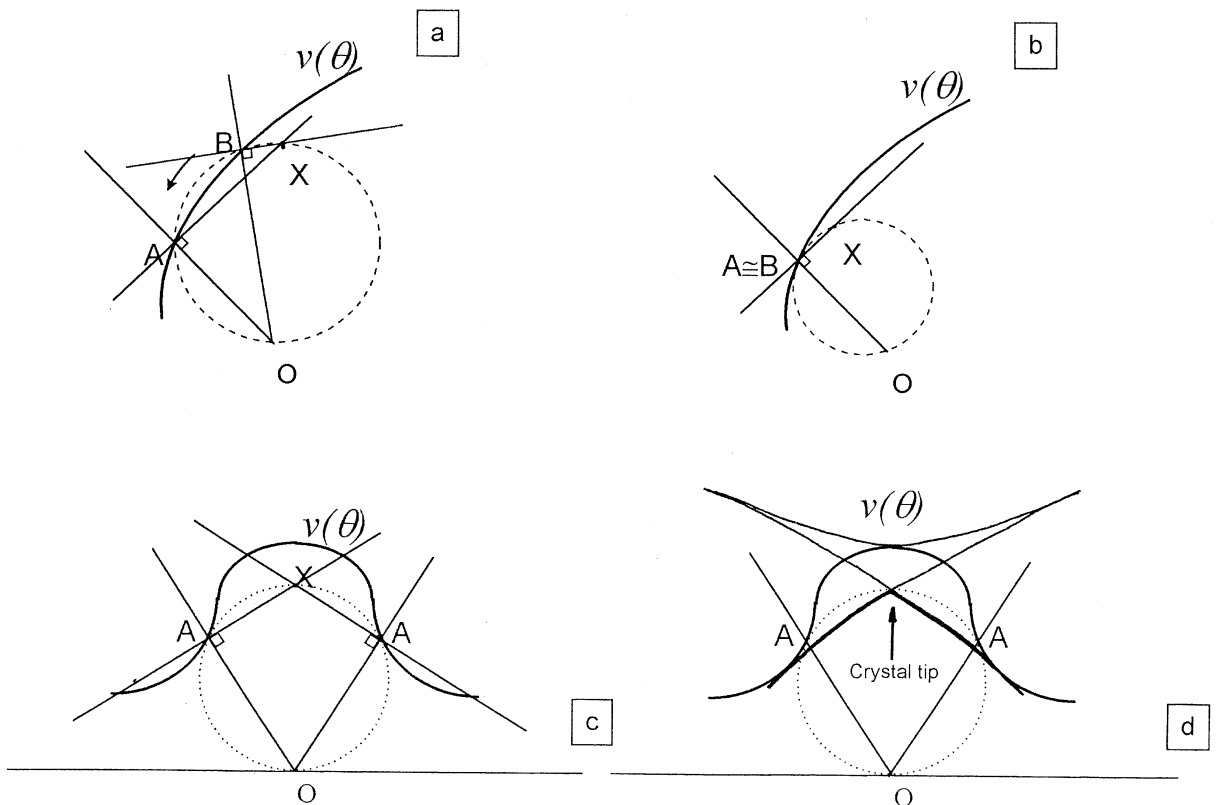


Fig. 4. Wulff construction showing why a sufficiently anisotropic crystal grows with a discontinuity at the apex. (a) The circle  $OABX$  goes through the origin  $O$  and two points  $A$  and  $B$  on the  $v(\theta)$  plot. The normals to  $v(\theta)$  at  $A$  and  $B$  meet at  $X$  which is diametrically opposite  $O$ . (b) If  $A \rightarrow B$  the circle touches  $v(\theta)$  and  $X$  is a candidate point for the crystal profile. (c) If a circle through  $O$  touches  $v(\theta)$  simultaneously at two points  $A, A'$ , and their common  $X$  is within the curve  $v(\theta)$ , there is a discontinuity at  $X$  in the slope of the crystal profile, which changes from tangent  $AX$  to  $A'X$ . (d) This can be seen if we use the construction in (b) to plot the points  $X$  continuously as  $A$  moves around  $v(\theta)$ ; the curve crosses itself at this point.

exposition of this interpretation of the Wulff construction. The argument, which is developed in more detail in the figure caption, shows that a discontinuity in the gradient of the profile (i.e. a sharp point) results if it is possible to draw a circle within  $v(\theta)$  which goes through the origin and touches the curve  $v(\theta)$  at two points. If this is so, then the angle jumps from one contact point to the other. Between these two angles, no data on angular dependences can be obtained experimentally. In the case of  $\text{NH}_4\text{Cl}$  this occurs, essentially, because of the higher angular frequency of  $\beta(\theta)$  once the kinetic term (3) becomes dominant.

#### 4. Growth in three dimensions: optical tomography on growing ice crystals

An experimental investigation using optical tomography studied the growth of ice crystals from supercooled water. Since the variation of refractive index with temperature  $dn/dT$  is very close to zero for water at  $T = 0^\circ\text{C}$  (water has maximum refractive index at  $0.1^\circ\text{C}$ ), heavy water was used for the experiments, since this has maximum refractive index at  $7^\circ\text{C}$ . Experiments carried out on ice crystals growing with a pyramidal morphology are described in detail by Braslavsky [17] in an accompanying paper. Here we shall discuss a more general question which the experiments help to answer. Many growing crystals tend to grow in the form of asymmetrical needles; this has been ob-

served with liquid crystals, helium, ice etc. (Fig. 5a), which are all anisotropic hexagonal crystals, having a considerable difference between the growth admittances along the hexagonal axis ( $c$ ) and normal to it ( $a$ ). However, the anisotropy itself does not explain the asymmetry of the needles, since symmetrically related orientations still have the same growth parameters. Following the construction shown in Fig. 4, we can see that the large difference in growth velocity along  $c$  and  $a$  leads to pointed crystals (Fig. 4d). One now asks whether the point is stable. Following the basic idea of the Mullins–Sekerka instability, one now supposes that

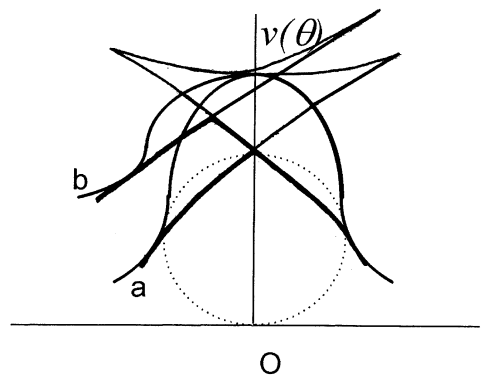


Fig. 6. Wulff diagrams showing orientation discontinuities at the tip of an anisotropically growing crystal. Curve (a) for  $v(\theta)$  has mirror symmetry, whereas (b) represents the case where the increased supercooling on the left has increased the growth velocities on that side.

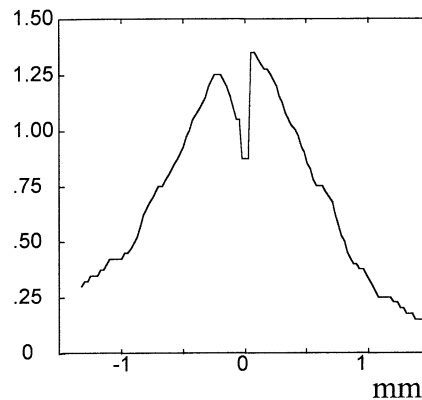
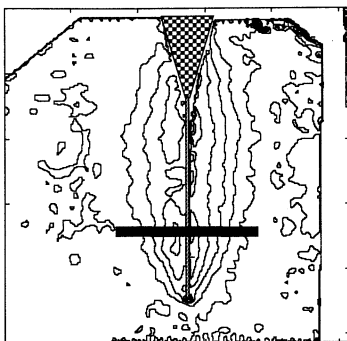


Fig. 5. The temperature map around an asymmetrically-growing ice crystal. (a) contour map; (b) section along the thick black line in (a).

there is a small fluctuation which increases the supercooling on one side, causing an increase in the velocity on that side. The Wulff construction then shows the crystal point to tilt to that side (Fig. 6). This situation is unstable since, as a result, the crystal growth axis deviates to the direction where the supercooling is greater which reinforces the increase in velocity that originally caused the tilt. Using the temperature maps of ice crystals, which show clearly where the heat emission is greatest, we can confirm that this is indeed the case (Fig. 5b).

## 5. Conclusions

In this article we have described briefly how imaging the concentration and temperature fields around growing crystals can give new insights which help to understand both morphology transitions and instabilities commonly observed during crystal growth.

## Acknowledgements

This work has been supported by the GIF (German–Israel Science Foundation) and by the Minerva Centre for Non-Linear Science.

## References

- [1] G. Wulff, *Z. Krist.* 34 (1901) 449.
- [2] C. Herring, *Phys. Rev.* 82 (1951) 87.
- [3] E.A. Brener, V.I. Mel'nikov, *Adv. Phys.* 40 (1991) 53.
- [4] Y. Pomeau, M. Ben-Amar, in: C. Godreche (Ed.), *Solids far from Equilibrium*, Ch. 4, Cambridge University Press, Cambridge, 1992.
- [5] J.S. Langer, H. Müller-Krumbhaar, *Acta Met.* 26 (1978) 1681.
- [6] R. Kupferman, O. Shochet, E. Ben-Jacob, *Phys. Rev. E* 40 (1994) 1005.
- [7] E. Brener, H. Müller-Krumbhaar, D. Temkin, *Phys. Rev. E* 54 (1996) 2714.
- [8] C.W. Bunn, H. Emmet, *Disc. Farad. Soc.* 5 (1949) 132.
- [9] E. Raz, S.G. Lipson, E. Polturak, *Phys. Rev. A* 40 (1989) 1088.
- [10] S. Kostianovski, S.G. Lipson, E. Ribak, *Appl. Opt.* 32 (1993) 4744.
- [11] I. Braslavsky, S.G. Lipson, *Physica A* 249 (1998) 190.
- [12] D. Verhoeven, *Appl. Optics* 32 (1993) 3736.
- [13] M. Kahlweit, *J. Crystal Growth* 5 (1969) 391.
- [14] E. Ben-Jacob, P. Garik, T. Mueller, D. Grier, *Phys. Rev. A* 38 (1988) 1370.
- [15] E.A. Brener, *Sov. Phys. JETP* 69 (1989) 133.
- [16] J. Maurer, P. Bouissou, B. Perrin, P. Tabeling, *Europhys. Lett.* 8 (1989) 67.
- [17] M. Elbaum, J.S. Wettlaufer, *Phys. Rev. E* 48 (1993) 3180.
- [18] A.A. Chernov, in: H.-J. Quessier (Ed.), *Modern Crystallography, III: Crystal Growth*, Springer, Berlin, 1984.
- [19] J.S. Wettlaufer, M. Jackson, M. Elbaum, *J. Phys. A* 27 (1994) 5967.